

# Towards a parameterization of lake biogeochemistry for the Earth System models

Victor Stepanenko<sup>1</sup>

<sup>1</sup>Lomonosov Moscow State University

## Contributors:

V.Yu.Bogomolov, V.N.Lykossov, E.M.Volodin, I.Mammarella,  
H.Miettinen, A.Ojala, T.Vesala, S.P.Guseva, A.Medvedev

5th workshop “Parameterization of Lakes in Numerical Weather Prediction and  
Climate Modelling”,  
Berlin, 19 October 2017

# Freshwaters in global carbon cycle

(Tranvik et al. 2009)

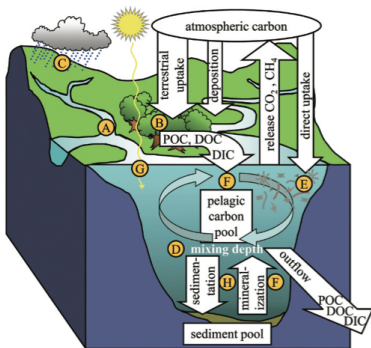


Fig. 2. Schematic diagram showing pathways of carbon cycling mediated by lakes and other continental waters. The letters correspond to rows in Table 1.

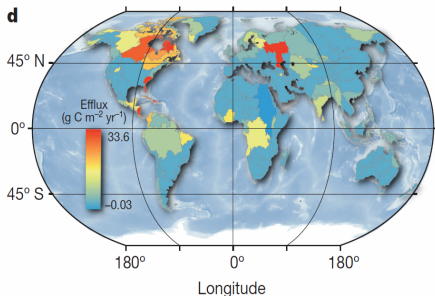
(Bastviken et al. 2011)

Latitude	Fluxes												Area (km <sup>2</sup> )
	Total open water			Ebullition			Diffusive			Stored			
	Emiss.	<i>n</i>	CV	Emiss.	<i>n</i>	CV	Emiss.	<i>n</i>	CV	Emiss.	<i>n</i>	CV	
Lakes													
>66°	6.8	17	72	6.4	17	74	0.7	60	37				288,318
>54°–66°	6.6	5	155	9.1	9	60	1.1	271	185	0.1	217	2649	1,533,084
25°–54°	31.6	15	127	15.8	15	177	4.8	33	277	3.7	36	125	1,330,264
<24°	26.6	29	51	22.2	28	54	3.1	29	97	21.3	1		585,536*
Reservoirs													
>66°	0.2 <sup>†</sup>												35,289
>54°–66°	1.0	24	176	1.8	2	140	0.2	4	93				161,352
25°–54°	0.7 <sup>‡</sup>												116,922
<24°	18.1	11	87										186,437
Rivers													
>66°	0.1	1											38,895
>54°–66°	0.2 <sup>†</sup>												80,009
25°–54°	0.3	20	302										61,867
<24°	0.9 <sup>‡</sup>												176,856
Sum open water	93.1	116		55.3	71		9.9	397		25.1	254		
Plant flux	10.2												
Sum all	103.3												

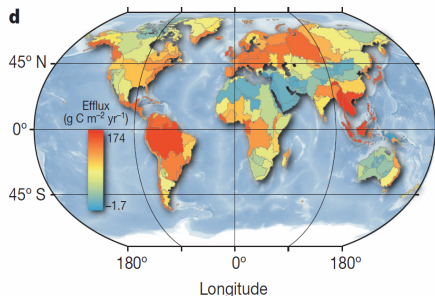
- Total freshwater methane emission is 104 Tg yr<sup>-1</sup>, i.e. 50% of global wetland emission (177-284 Tg yr<sup>-1</sup>, IPCC, 2013)
- greenhouse warming potentials from freshwater-originating CO<sub>2</sub> and CH<sub>4</sub> are roughly equal

# CO<sub>2</sub> emissions by lakes and rivers

Raymond et al., 2013, Nature



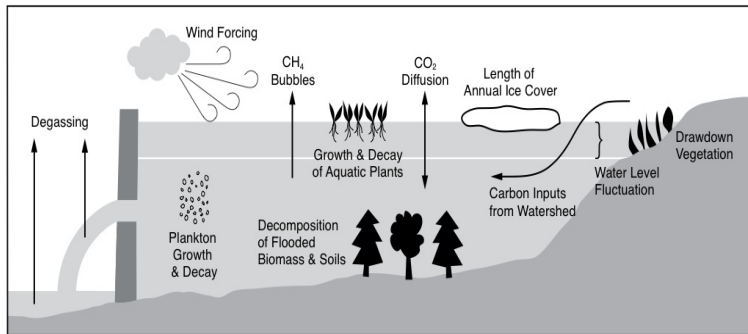
Lakes



Rivers

- global emission of CO<sub>2</sub> by freshwaters is 2.1 Pg C yr<sup>-1</sup>
- lake emission is 0.3 Pg C yr<sup>-1</sup>, river emissions is 1.8 Pg C yr<sup>-1</sup>
- significant contribution of Volga hydropower reservoirs

# Emission of greenhouse gases from reservoirs



- Artificially flooded ecosystems are imposed to both aerobic (producing CO<sub>2</sub>) and anaerobic (producing CH<sub>4</sub>) degradation
- Compared to natural lakes there is an additional pathway of gases that is through turbines



# Global warming of lakes

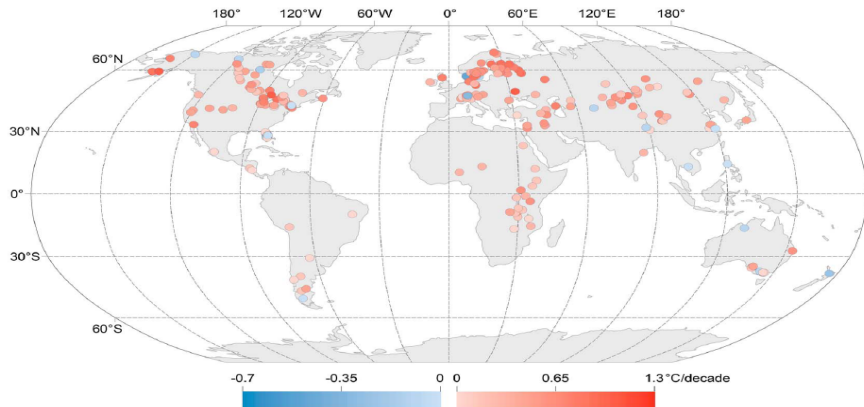


**Figure 1.** Map of trends in lake summer surface temperatures from 1985 to 2009. Most lakes are warming, and there is large spatial heterogeneity in lake trends. Note that the magnitudes of cooling and warming are not the same.

The majority of lakes are warming at a rate higher than  $T_{2m}$ .

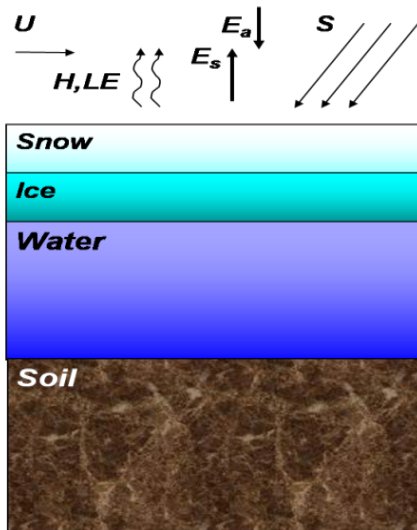
O'Reilly et al., 2015, GRL, doi:10.1002/ 2015GL066235

# 1D lake model framework

1D equations result from boundary-layer approximation

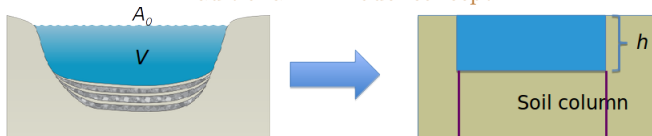
- 1D heat and momentum equations
- $k - \epsilon$  turbulence closure
- Monin-Obukhov similarity for surface fluxes
- Beer-Lambert law for shortwave radiation attenuation
- Momentum flux partitioning between wave development and currents (Stepanenko et al., 2014)
- Soil heat and moisture transfer including phase transitions
- Multilayer snow and ice models

1D concept does not suffice the greenhouse gas modeling task, as it does not take into account differences between  $CH_4$  &  $CO_2$  emissions at deep and shallow sediments



# 1D<sup>+</sup> framework

Traditional 1D model concept



1D<sup>+</sup> model concept

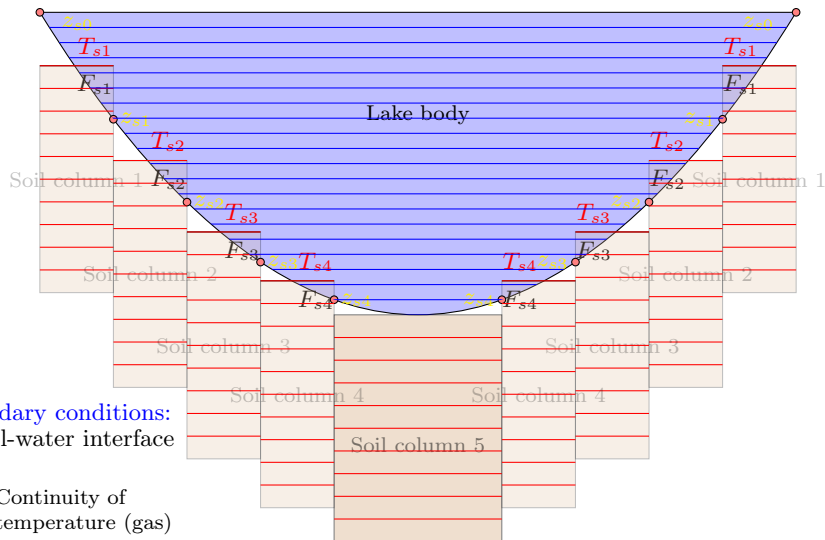
- 1D<sup>+</sup> model includes friction, heat and mass exchange at the lateral boundaries
- Heat, moisture and gas transfer are solved for each soil column independently



In 1D<sup>+</sup> model horizontally averaged quantity  $f$  obeys the equation:

$$\frac{\partial f}{\partial t} = \frac{1}{A} \frac{\partial}{\partial z} \left[ A k_f \frac{\partial f}{\partial z} \right] + F(z, t, f, A) + H_f \frac{1}{A} \frac{dA}{dz}.$$

# Coupling heat transport in water and soil



Boundary conditions:  
at soil-water interface

- Continuity of temperature (gas)
- Continuity of flux

# 1D equations for enclosed basins

Horizontally-averaged 3D equations for basic prognostic quantities:

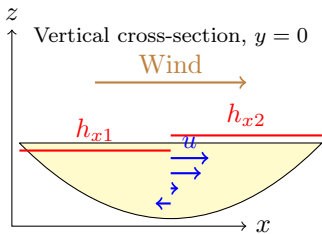
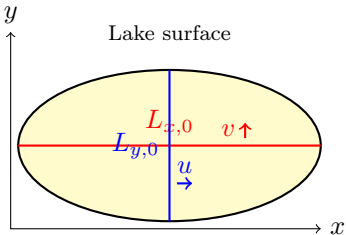
$$c_w \rho_w \frac{\partial \bar{T}}{\partial t} = \dots \frac{1}{A} \frac{\partial}{\partial z} \left( A (\lambda_m + c_w \rho_w \nu_T) \frac{\partial \bar{T}}{\partial z} \right) -$$
$$- \frac{1}{A} \frac{\partial A \bar{S}}{\partial z} + \frac{1}{A} \frac{dA}{dz} [S_b + F_{T,b}(z)], \quad - \text{heat conservation equation} \quad (1)$$

$$\frac{\partial \bar{u}}{\partial t} = \dots - \overline{\left( \frac{1}{\rho_w} \frac{\partial p}{\partial x} \right)} + \frac{1}{A} \frac{\partial}{\partial z} \left( A (\nu + \nu_m) \frac{\partial \bar{u}}{\partial z} \right) +$$
$$+ \frac{1}{A} \frac{dA}{dz} F_{u,b}(z) + f \bar{v}, \quad - \text{momentum equation for x-speed component} \quad (2)$$

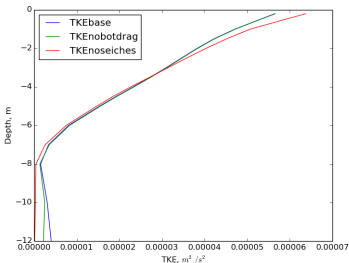
$$\frac{\partial \bar{v}}{\partial t} = \dots - \overline{\left( \frac{1}{\rho_w} \frac{\partial p}{\partial y} \right)} + \frac{1}{A} \frac{\partial}{\partial z} \left( A (\nu + \nu_m) \frac{\partial \bar{v}}{\partial z} \right) +$$
$$+ \frac{1}{A} \frac{dA}{dz} F_{v,b}(z) - f \bar{u} \quad - \text{momentum equation for y-speed component} \quad (3)$$

# Barotropic pressure gradient and seiches

Barotropic (surface) seiches are lake surface and related velocity oscillations after strong wind events.



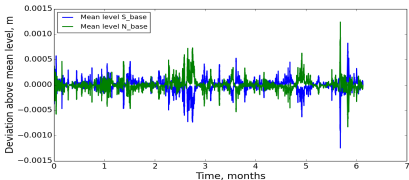
Turbulent kinetic energy profile (modeled), June 2013, Kuivajarvi Lake, seiches produce TKE near bottom



Mass conservation 
$$\begin{cases} \frac{dh_N}{dt} A_0(t) = -\frac{dh_S}{dt} A_0(t) = 2 \int_0^1 v L_{W-E} h d\xi, \\ \frac{dh_E}{dt} A_0(t) = -\frac{dh_W}{dt} A_0(t) = 2 \int_0^1 u L_{S-N} h d\xi, \end{cases}$$

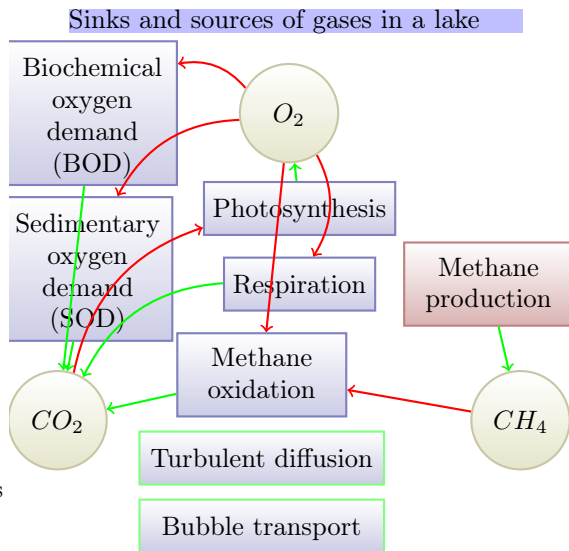
Barotropic pressure gradient force 
$$\begin{cases} g \frac{\partial \bar{h}_S}{\partial x} \approx \frac{g\pi^2}{4} \frac{h_E - h_W}{L_{W-E,0}}, \\ g \frac{\partial \bar{h}_S}{\partial y} \approx \frac{g\pi^2}{4} \frac{h_N - h_S}{L_{S-N,0}}. \end{cases}$$

Surface oscillations in the model



# Biogeochemical processes in the model

- Photosynthesis, respiration and BOD are empirical functions of temperature and Chl-a (Stefan and Fang, 1994)
- Oxygen uptake by sediments (SOD) is controlled by  $O_2$  concentration and temperature (Walker and Snodgrass, 1986)
- Methane production  $\propto P_0 q_{10}^{T-T_0}$ ,  $P_0$  is calibrated (Stepanenko et al., 2011)
- Methane oxidation follows Michaelis-Menten equation



# Model validation for Seida Lake

Guseva et al., Geogr. Env. Sust., 2016

## Seida lake location



## Bubble flux (starting from 01.07.2007)

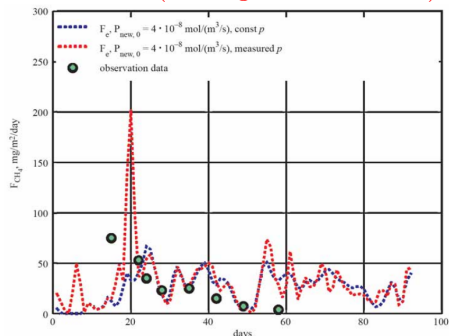


Table 3. Methane production rate constant  $P_{new, 0}$  in other studies

$P_{new, 0} \text{ (mol} \cdot \text{m}^{-3} \cdot \text{s}^{-1}\text{)}$	Source
$3.0 \cdot 10^{-8}$	Lake Kuivajärvi, Finland [Stepanenko et al., 2016]
$2.55 \cdot 10^{-8}$	Shuchi Lake, North Eastern Siberia, Russia [Stepanenko et al., 2011]
$8.3 \cdot 10^{-8} - 1.6 \cdot 10^{-7}$	High latitude wetlands [Walter & Heimann, 2000]
$4.0 \cdot 10^{-8}$	Lake at the Seida site, current study



# Kuivajärvi Lake (Finland)

- Mesotrophic, dimictic lake
- Area  $0.62 \text{ km}^2$  (length 2.6 km, modal fetch 410 m)
- Altitude 142 m a.s.l.
- Maximal depth 13.2 m, average depth 6.4 m, depth at the point of measurements 12.5 m
- Catchment area  $9.4 \text{ km}^2$

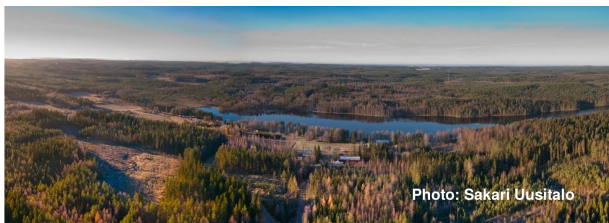
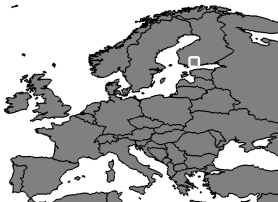
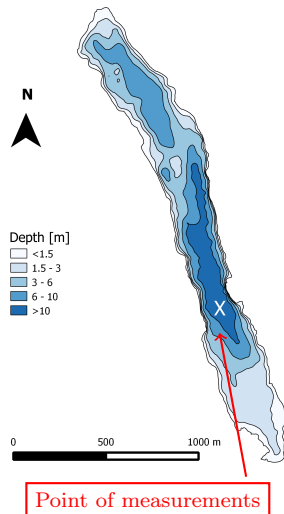


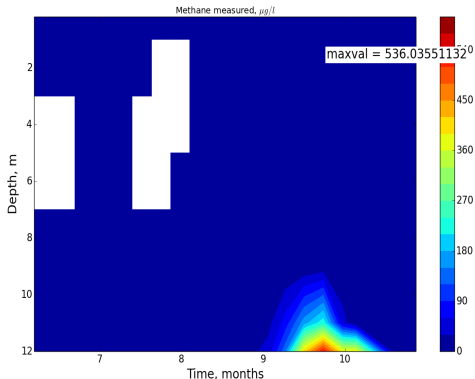
Photo: Sakari Uusitalo



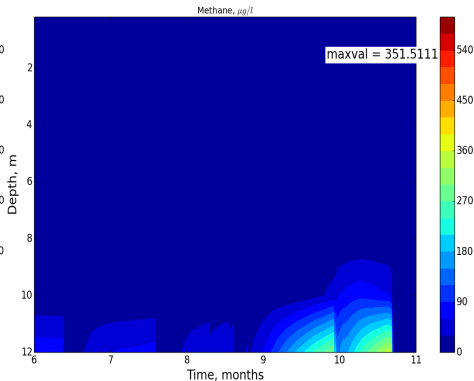
# Methane

Stepanenko et al., Geosci. Mod. Dev., 2016

Measurements



Model

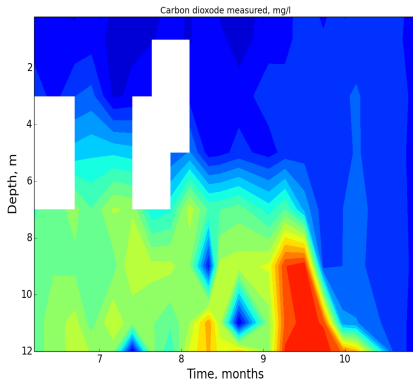


- Methane starts to accumulate near bottom in the late summer when oxygen concentration drops to low values
- Surface methane concentration is very small leading to negligible diffusive flux to the atmosphere, consistent with measurements

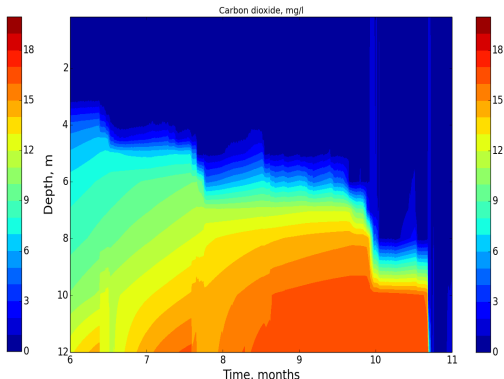
# Carbon dioxide concentration

Stepanenko et al., Geosci. Mod. Dev., 2016

Measurements



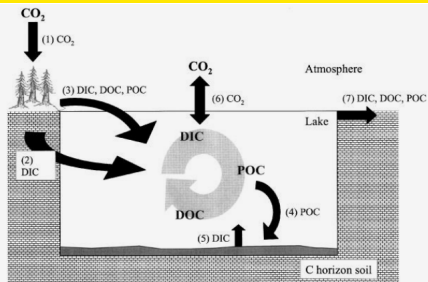
Model



- Seasonal pattern is simulated realistically: carbon dioxide is **consumed** by photosynthesis in the mixed layer and **produced** in the thermocline and hypolimnion by aerobic organics decomposition
- Sudden  $CO_2$  increase prior to autumn overturn is absent in the model

# Further development: dissolved and particulate carbon

Adopting approach from Hanson et al., 2004



## Extended biogeochemical model

$$\frac{\partial C_{CH_4}}{\partial t} = Dif_A(C_{CH_4}) + B_{CH_4} - O_{CH_4}, \quad (1)$$

$$\frac{\partial C_{O_2}}{\partial t} = Dif_A(C_{O_2}) + B_{O_2} + P_{O_2} - R_{O_2} - D_{O_2} - S_{O_2} - O_{O_2}, \quad (2)$$

$$\frac{\partial C_{DIC}}{\partial t} = Dif_A(C_{DIC}) + B_{CO_2} - P_{CO_2} + R_{CO_2} + D_{CO_2} + S_{CO_2} + O_{CO_2}, \quad (3)$$

$$\frac{\partial \rho_{DOC}}{\partial t} = Dif(\rho_{DOC}) + E_{POCL} - D_{DOC}, \quad (4)$$

$$\frac{\partial \rho_{POCL}}{\partial t} = Dif(\rho_{POCL}) + P_{POCL} - R_{POCL} - E_{POCL} - D_{h,POCL}, \quad (5)$$

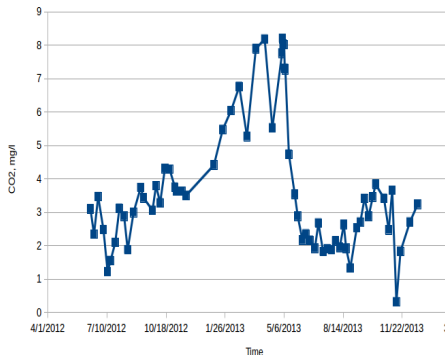
$$\frac{\partial \rho_{POCD}}{\partial t} = Dif(\rho_{POCD}) - \frac{w_g}{h} \frac{\partial \rho_{POCD}}{\partial \xi} - D_{POCD} + D_{h,POCL}. \quad (6)$$

- The Hanson et al. model is reformulated to explicitly reproduce vertical distribution of DOC, POCL, POCD (instead of using mixed-layer and hypolimnion pools, as in original paper)
- The horizontal influx from catchment is included given the inlet measurement data

# Surface carbon dioxide concentration

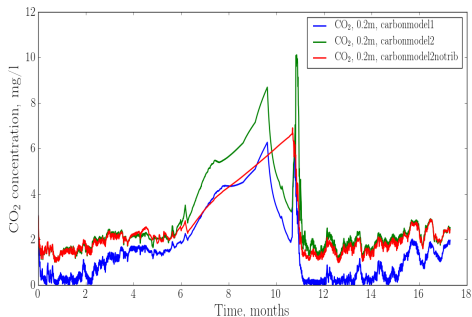
Kuivajarvi Lake, June 2012 – December 2013

Measurements



Model

Old carbon model, New carbon model,  
New carbon model with NO inflow



Surface CO<sub>2</sub> concentrations (~8 mg/l in winter, 2-3 mg/l in summer) are well captured by the model – dynamics of DOC and POC may be crucial to simulate lake-atmosphere CO<sub>2</sub> exchange

# Earth system model INMCM

Developed by Russian consortium lead by Institute of Numerical Mathematics

Model includes:

- Atmospheric dynamics
- Soil and vegetation
- Oceanic dynamics, including sea ice
- Carbon cycle
- Aerosol module
- Some electric phenomena

Participated in: CMIP3(2003-2004), CMIP5 (2010-2011)

Participates: CMIP6 (2017-2018)

Current versions:

- INM-CM4-8: Atmosphere 2x1.5 degrees, 30 levels, the uppermost level at 10hPa. Ocean: 1x0.5 degrees, 40 levels
- INM-CM5-0: Atmosphere 2x1.5 degrees, 73 levels, the uppermost level at 0.2 hPa. Ocean: 0.5x0.25 degrees, 40 levels.
- INM-CM5-H: Atmosphere 2x1.5 degrees, 73 levels, the uppermost level at 0.2 hPa. Ocean: 0.5x0.25 degrees, 40 levels.

# Incorporation of LAKE model into LSM

## Land surface model:

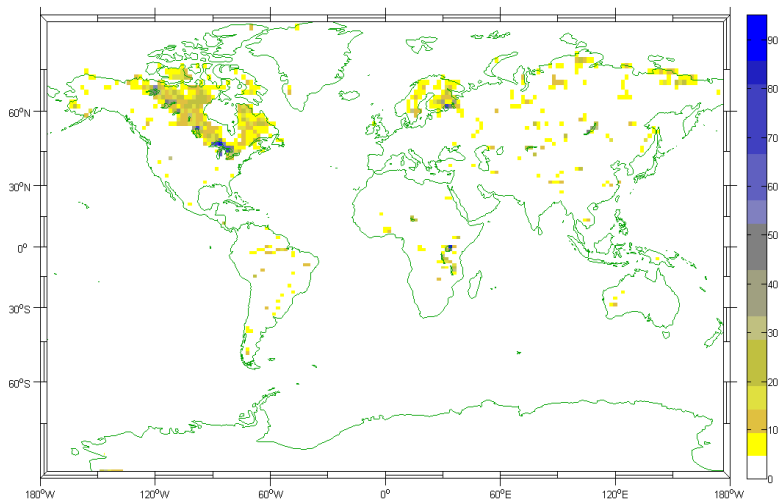
- tile approach including: bare soil, vegetation, snow and inland waters
- inland waters are represented by soil with the surface properties of water
- time step is 1 hour

## LAKE model modifications:

- $k - \epsilon$  model does not allow more than 1-10 min timesteps  $\rightarrow$  changed to Hendersson-Sellers diffusivity + convective mixing
- lake morphometry effects excluded
- surface flux scheme from LSM is applied

# Global lake coverage at INMCM model grid

Extracted from Choulga et al., 2014 database

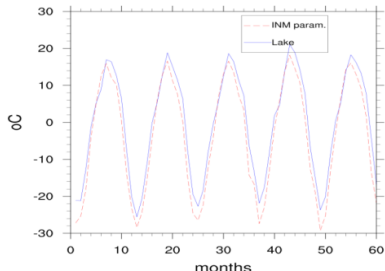




# New lake parameterization vs. old parameterization

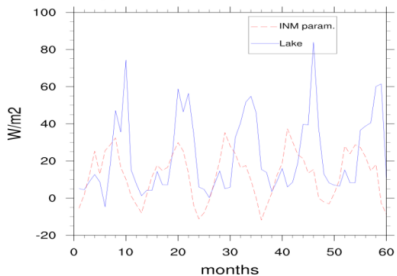
Exemplified for lake tile of cells containing Lake Baikal

Average monthly values of Surface temperature

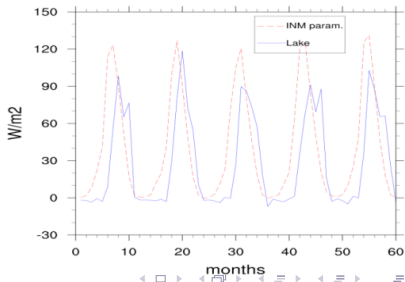


The maximal values of lake surface temperature, sensible and latent heat flux are shifted towards autumn

Average monthly values of Sensible heat flux



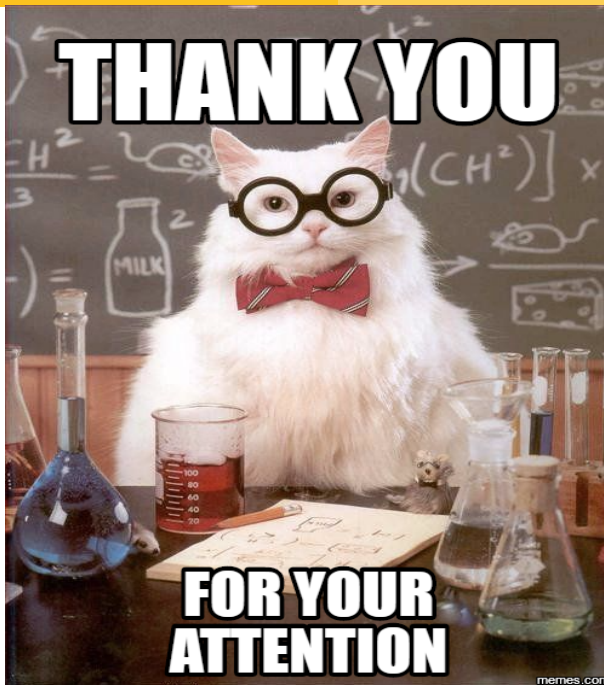
Average monthly values of Latent heat flux



# Outlook

- LAKE model was successfully tested in terms of  $\text{CH}_4$  emissions at three lakes: Shuchi (North-Eastern Siberia, Stepanenko et al., 2011), Seida (North of European Russia), Kuivajarvi (Finland)
- introducing of POC and DOC dynamics in lakes improves  $\text{CO}_2$  simulations for Kuivajarvi Lake
- LAKE model has been incorporated to land surface scheme of INMCM Earth system model (+1 ESM with lake parameterization), the temperature and surface fluxes are reasonably reproduced but ...
- further performance testing is needed, involving satellite-derived surface temperature for biggest lakes and feedbacks from lakes on surface atmospheric fields
- lake biogeochemistry modeling in LSM is coming... but new external datasets and global validation data would be needed

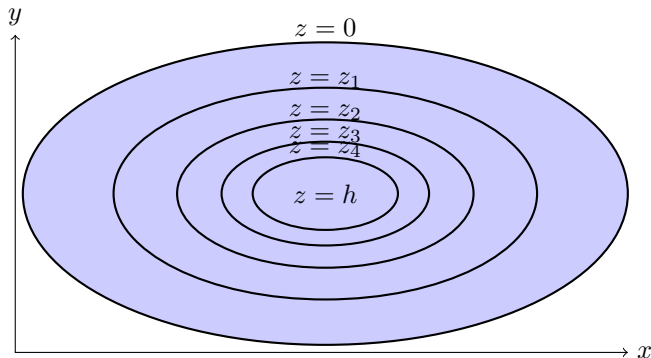
The work is supported by grants RSF 17-17-01210 and RFBR 17-05-01165



# Soil columns in the model

## Horizontal projection

Soil columns are geometric figures of the same vertical dimension and with horizontal sections confined by sequential isobaths:



# Freshwaters in global carbon cycle

(Tranvik et al. 2009)

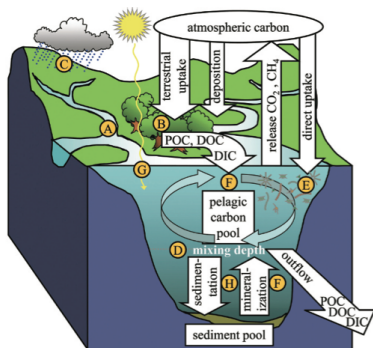


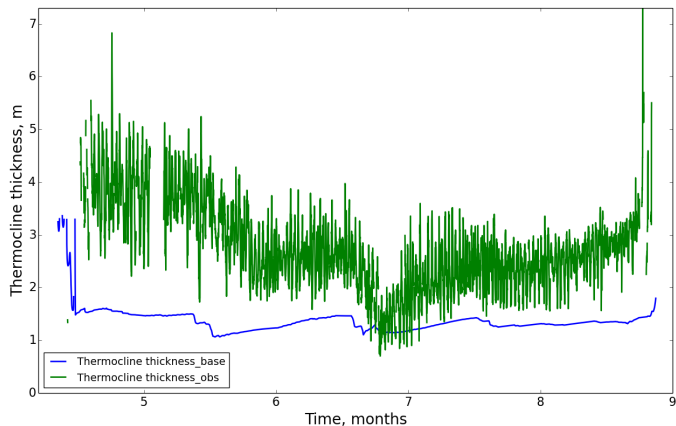
Fig. 2. Schematic diagram showing pathways of carbon cycling mediated by lakes and other continental waters. The letters correspond to rows in Table 1.

(Bastviken et al. 2011)

Latitude	Fluxes												Area (km <sup>2</sup> )
	Total open water			Ebullition			Diffusive			Stored			
	Emiss.	<i>n</i>	CV	Emiss.	<i>n</i>	CV	Emiss.	<i>n</i>	CV	Emiss.	<i>n</i>	CV	
Lakes													
>66°	6.8	17	72	6.4	17	74	0.7	60	37				288,318
>54°–66°	6.6	5	155	9.1	9	60	1.1	271	185	0.1	217	2649	1,533,084
25°–54°	31.6	15	127	15.8	15	177	4.8	33	277	3.7	36	125	1,330,264
<24°	26.6	29	51	22.2	28	54	3.1	29	97	21.3	1		585,536*
Reservoirs													
>66°	0.2 <sup>†</sup>												35,289
>54°–66°	1.0	24	176	1.8	2	140	0.2	4	93				161,352
25°–54°	0.7 <sup>‡</sup>												116,922
<24°	18.1	11	87										186,437
Rivers													
>66°	0.1	1											38,895
>54°–66°	0.2 <sup>†</sup>												80,009
25°–54°	0.3	20	302										61,867
<24°	0.9 <sup>‡</sup>												176,856
Sum open water	93.1	116		55.3	71		9.9	397		25.1	254		
Plant flux	10.2												
Sum all	103.3												

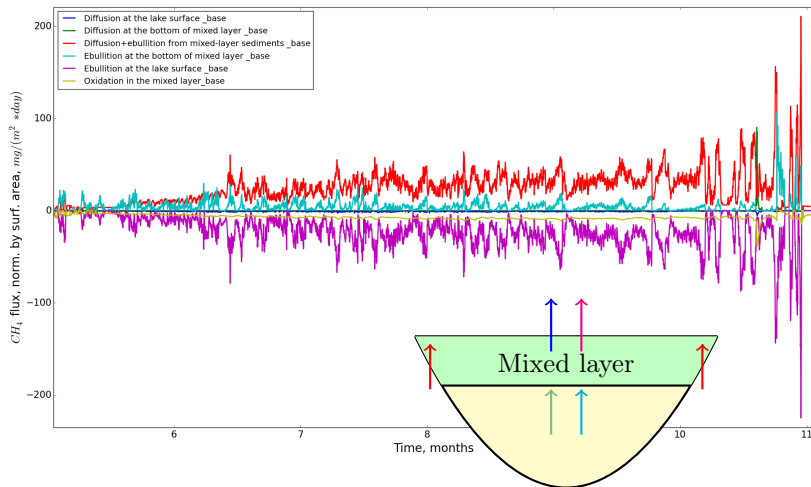
- Total freshwater methane emission is 104 Tg  $yr^{-1}$ , i.e. 50% of global wetland emission (177–284 Tg  $yr^{-1}$ , IPCC, 2013)
- greenhouse warming potentials from freshwater-originating  $CO_2$  and  $CH_4$  are roughly equal

# Thermocline thickness



Thermocline thickness is defined as a depth difference between 8 °C and 14 °C isotherms

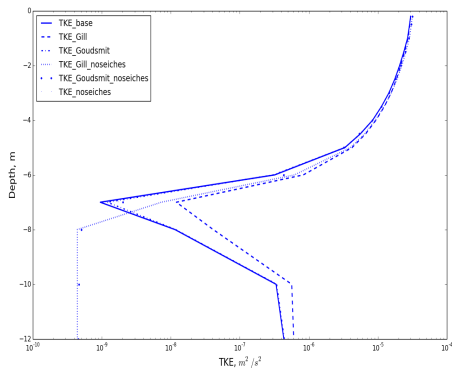
# Methane budget in the surface mixed layer



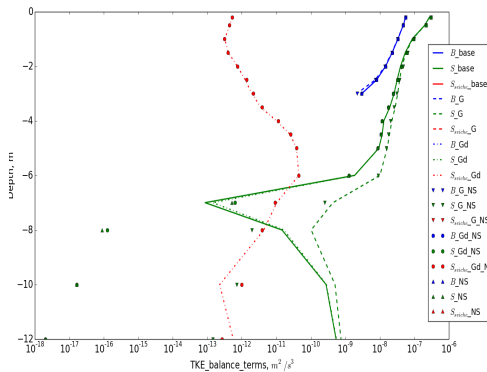
The diffusive flux through thermocline is negligible compared to other terms

# TKE profiles

TKE



TKE balance terms



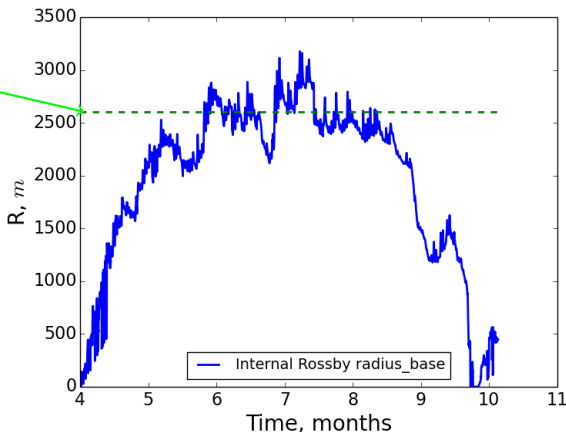


# Significance of Coriolis force for Kuivajärvi Lake

$$\text{Rossby deformation number, } Ro = \frac{NH}{f} \approx \frac{\sqrt{g\rho_0^{-1}\Delta\rho} h_{ML}}{f}$$

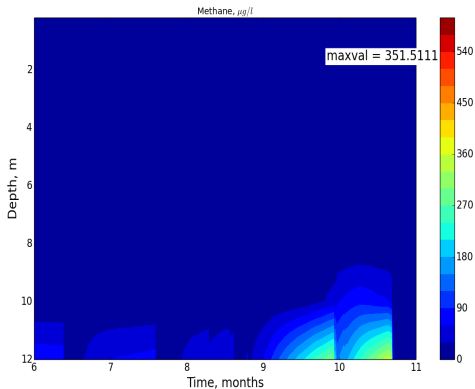
The lake's length

Rotational effects  
are comparable  
with those of  
stratification.

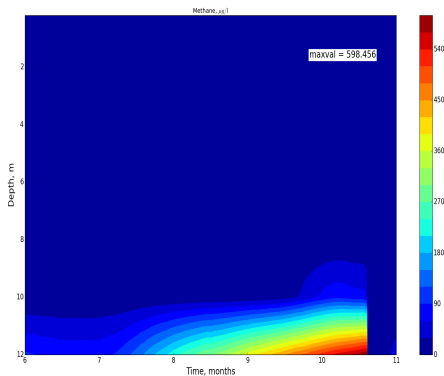


# The effect of barotropic seiches on methane

Control simulation



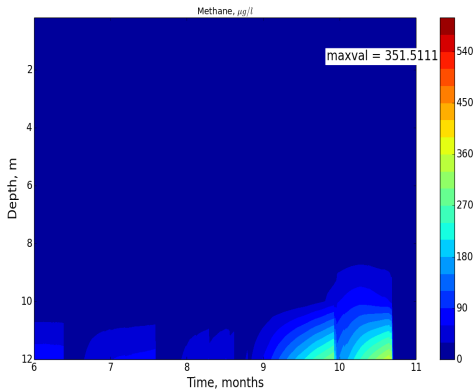
Seiches excluded



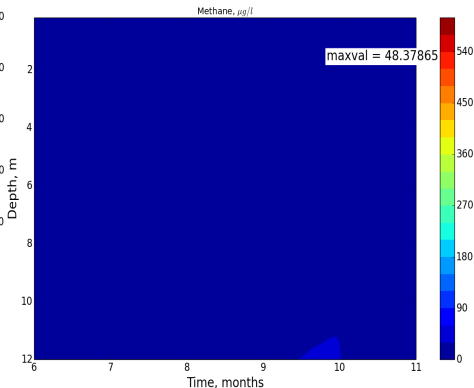
Neglecting barotropic seiches leads to  $TKE \approx 0$  below thermocline, less oxygen flux from above and earlier accumulation of methane near bottom

# Effect of weak turbulent mixing in the thermocline

Control simulation



Increased minimal  
diffusion coefficient ( $10 * \lambda_{w0}$ )



Oxygen diffuses downwards, oxidizing methane

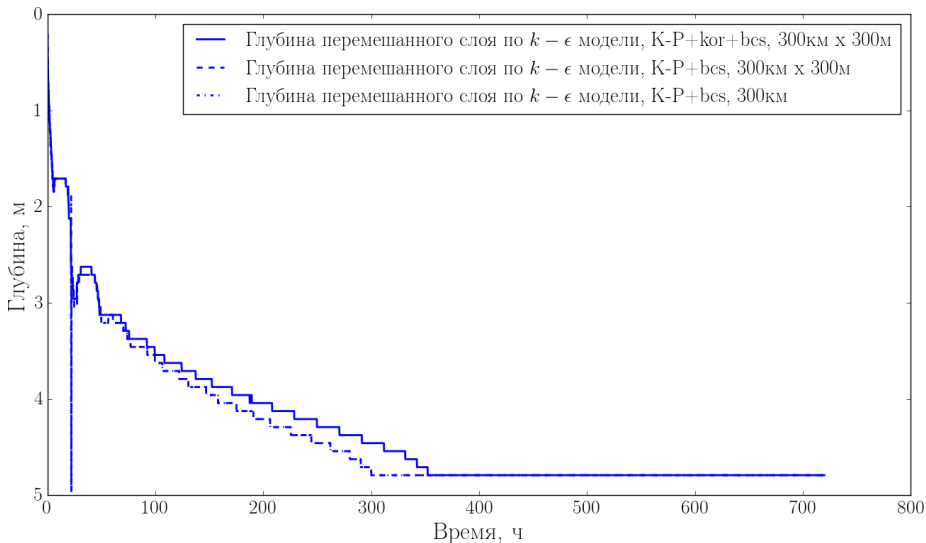


Figure: Эволюция глубины перемешанного слоя в эксперименте К.-Ф., дополненном учетом силы Кориолиса и параметризацией бароклинных сейш (результаты моделирования), при горизонтальных размерах озера:

300 км x 300 м и 300 км x 300 км

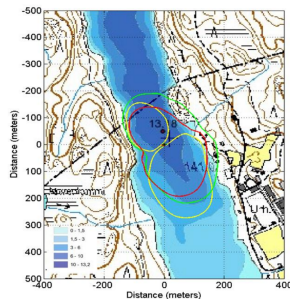
# Observations

- Conducted since 2009 by University of Helsinki
- Ultrasonic anemometer USA-1, Metek GmbH
- Enclosed-path infrared gas analyzers, LI-7200, LI-COR Inc.
- Four-way net radiometer (CNR-1)
- relative humidity at the height of 1.5 m (MP102H-530300, Rotronic AG)
- thermistor string of 16 Pt100 resistance thermometers (depths 0.2, 0.5, 1.0, 1.5, 2.0, 2.5, 3.0, 3.5, 4.0, 4.5, 5.0, 6.0, 7.0, 8.0, 10.0 and 12.0 m)
- Turbulent fluxes were calculated from 10 Hz raw data by EddyUH software

Measurement raft



Footprint of the raft measurements



# Internal seiche mixing parameterization in $k - \epsilon$ model

Goudsmit et al. 2002

- Shear production is generalized to include seiches  $P = \nu_t M^2 + P_s$ ;

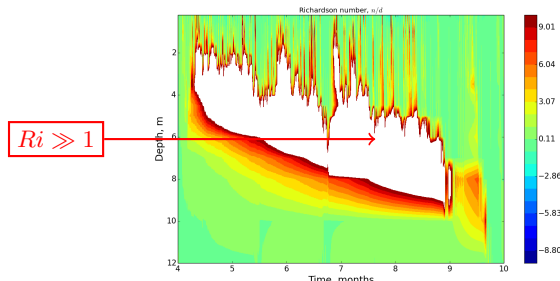
- TKE production by seiche-induced shear at lake's margins

$$P_s = -\frac{1-C_{diss}\sqrt{C_{d,bot}}}{\rho_w c A_b} \gamma \frac{1}{A} \frac{dA}{dz} N^2 E_s^{3/2}, \quad E_s - \text{seiche energy};$$

- Seiche energy is derived from wind forcing:  $\frac{dE_s}{dt} = \alpha A_0 \rho_a C_d (u^2 + v^2)^{3/2} - \gamma E_s^{3/2}$

- Stationary Richardson number (Burchard, 2002) may be derived for this case as

$$Ri_{st} = \frac{Pr \Delta c_{\epsilon 21}}{\Delta c_{\epsilon 23} - \nu_0^{-1} Pr C_s \Delta c_{\epsilon 21} (u^2 + v^2)^{3/2}} \approx 0.30 \text{ for typical wind speed}$$

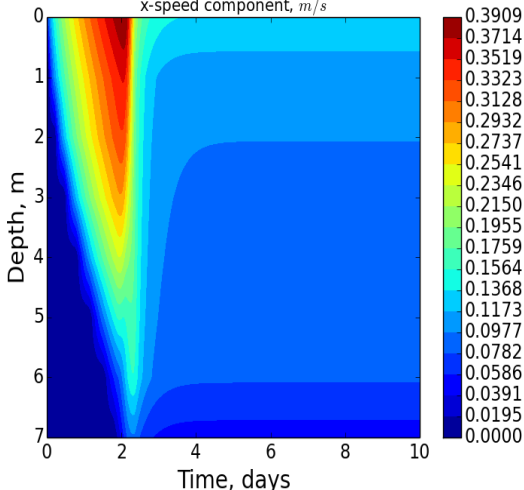


# Kato-Phillips experiment

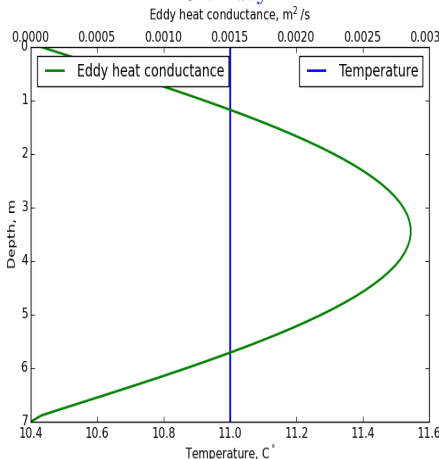
- no heat and radiation flux at the top and bottom boundaries
- constant surface wind stress  $0.01 \text{ N/m}^2$
- linear stable initial temperature profile,  $2 \text{ K/m}$
- no morphometry
- no rotation
- depth 7 m, 60 vertical computational layers
- 10 days of the model integration

# Kato-Phillips experiment results: Standard k- $\epsilon$ model

Time-depth distribution of velocity  
x-speed component, m/s



Temperature and eddy conductivity profiles  
9-th day



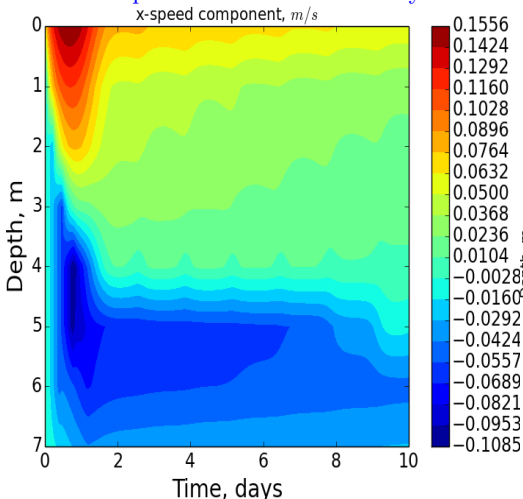
the deepening of the mixed layer follows well the known formula  $H_{ML} = 1.05 u_{*w} N_0^{-1/2} t^{1/2}$  (Price, 1979)

After complete mixing of temperature the flow is classical Couette flow

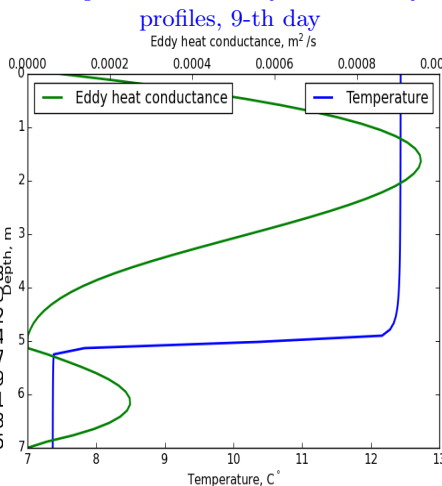


# Kato-Phillips experiment: $k$ - $\epsilon$ model + barotropic seiches

Time-depth distribution of velocity



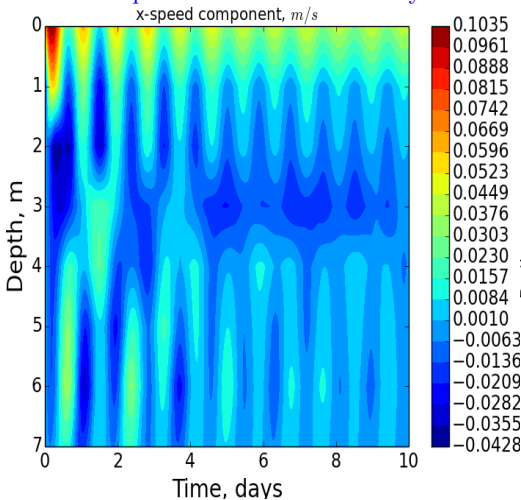
Temperature and eddy conductivity



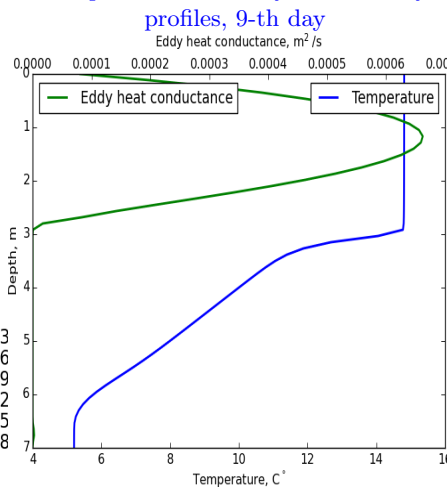
The bottom return flow creates another mixing layer, having very thin extremely stratified interface with the upper one

# Kato-Phillips experiment: $k$ - $\epsilon$ model + baroclinic seiches

Time-depth distribution of velocity

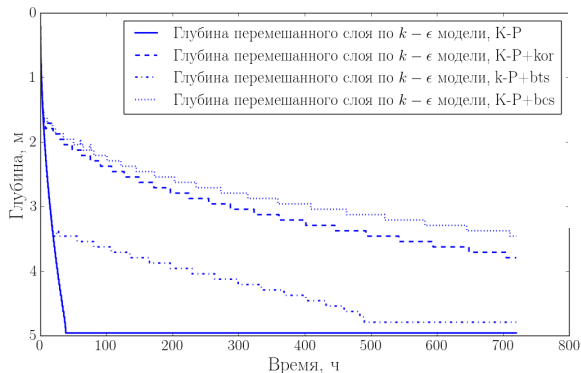


Temperature and eddy conductivity



The response of velocity to wind stress is waves, with dominating 1-st vertical mode,  $\sim 1$  day period. The thermocline is preserved, with both surface and bottom mixed layer present

# Mixed-layer depth



К-П – Kato-Phillips experiment,

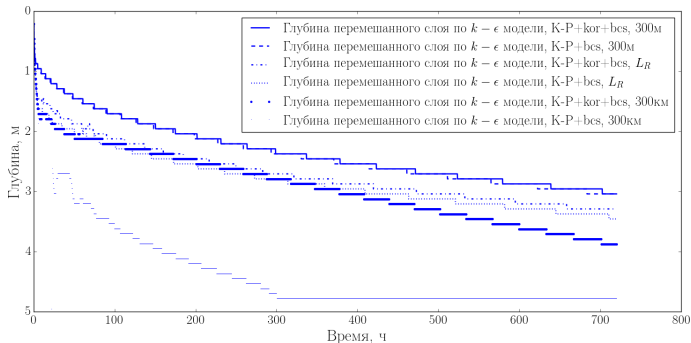
К-П+kor – Kato-Phillips experiment with Coriolis force,

К-П+bts – Kato-Phillips experiment with barotropic seiches,

К-П+bcs – Kato-Phillips experiment with baroclinic seiches

- Rotation and seiching impose similar suppressing effect on vertical mixing
- Barotropic seiche parameterization is not enough to produce "correct" mixing

# Mixed-layer depth



Kato-Phillips experiment with Coriolis force and baroclinic seiches at different lake sizes:

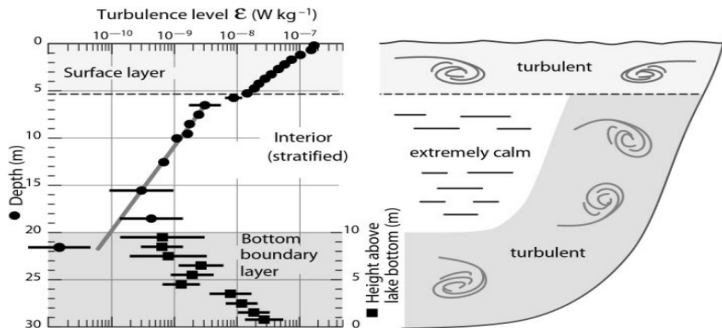
300 m $\times$ 300 m.  $L_R \times L_R$  and 300 km $\times$ 300 km ( $L_R \approx 2.77$  km)

- Coriolis force plays significant role in mixing compared to seiching only for the lake size  $L \gg L_R$
- The effect of Coriolis force for very large lakes is similar in magnitude to that of seiching for small lakes

# Why the mixing is suppressed by rotation and seiching?

- In classical Kato-Phillips setup, the friction is zero at the base of mixed layer, leading to continuous increase of total momentum in mixed layer (under constant momentum flux from the atmosphere), the shear production of TKE and mixed-layer deepening until complete mixing of temperature and achieving stationary Couette flow (where the momentum flux at the top is compensated by friction at the bottom)
- In both cases of rotation and seiching quasi-stationary oscillatory velocity patterns are established where Coriolis and pressure gradient terms (respectively) "consume" the constant momentum flux from the atmosphere

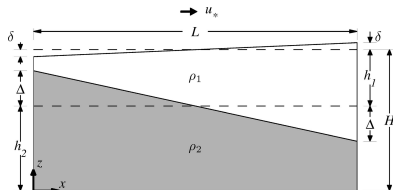
# Пограничные слои в водоемах (данные наблюдений)



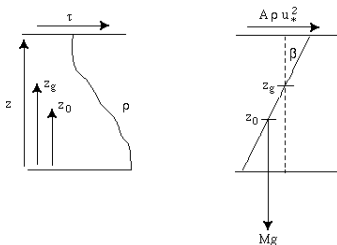
- верхний перемешанный слой – эпиминион: ТКЕ генерируется в основном за счет сдвига скорости ( $\sim$  напряжение трения)
- средний слой – металиминион (термоклин): очень устойчиво стратифицированный
- нижий слой – гипolimнион: генерация ТКЕ за счет сдвига внутренних циркуляций (сейши, волн Кельвина)

# Критерий справедливости одномерного приближения

Показано на примере оз.Куйваярви (Финляндия)



Shintani et al., 2010



Imerito, 2015

Wedderburn  
number

$$W = \frac{g \Delta \rho h_1^2}{\rho_0 u_*^2 L}$$

$$W_{cr} = \frac{1}{2}$$

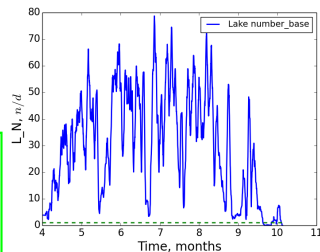
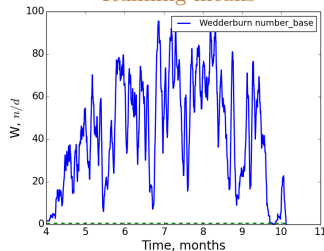
Lake number

$$L_N = \frac{2(z_m - z_v)V\rho_0 g h_1}{z_v \tau A_0 L}$$

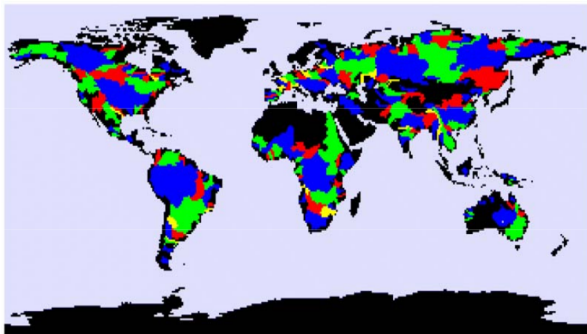
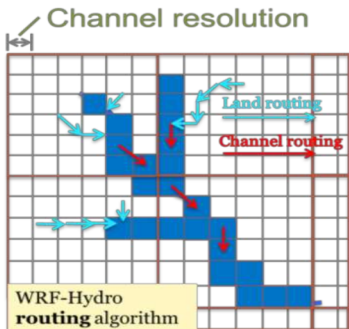
$$L_{N,cr} = 1$$

Thermocline  
displacement is  
negligible compared  
to mixed-layer depth

Running means



# Схемы маршрутизации водотоков (на примере TRIP)



- Вычислительно простые схемы, достаточные для воспроизведения средних расходов
- Диагностические формулы для расхода рек -> не воспроизводят экстремальные явления
- Нет расчета термодинамики и льдообразования
- Не учитываются биогеохимические процессы



# Модели водоема в климатических моделях и системах прогноза погоды

<b>Модель климата/прогноза погоды</b>	<b>Модель водоема</b>
IFS (ECMWF)	FLake
UKMO (MetOffice)	FLake
COSMO (European Consortium)	FLake
HIRLAM (European Consortium)	FLake
CESM (US consortium)	CLM-LISSS4
CRCM (Canada)	Flake/Hostetler
WRF (Penn SU)	FLake
...	...

# Модель пузырька

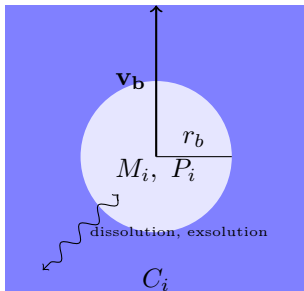
For shallow lakes (several meters), bubbles reach water surface not affected, for deeper lakes bubble dissolution has to be taken into account.

- Five gases are considered in a bubble:  $CH_4$ ,  $CO_2$ ,  $O_2$ ,  $N_2$ ,  $Ar$
- Bubbles are composed of  $CH_4$  and  $N_2$  when they are emitted from sediments
- The velocity of bubble,  $v_b$ , is determined by balance between buoyancy and friction
- The molar quantity of  $i$ -th gas in a bubble,  $M_i$ , changes according to gas exchange equation (McGinnis et al.,

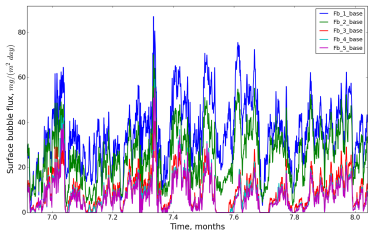
$$\frac{dM_i}{dt} = v_b \frac{\partial M_i}{\partial z} = -4\pi r_b^2 K_i (H_i(T)P_i - C_i).$$

- Gas exchange with solution is included in conservation equation for  $i$ -th gas :

$$\frac{\partial C_i}{\partial t} = \frac{1}{A} \frac{\partial}{\partial z} A k \frac{\partial C_i}{\partial z} + \frac{1}{A} \frac{\partial A B_{C_i}}{\partial z} + F(z, t, C_i, A) + (H_{C_i} - B_{C_i, b}) \frac{1}{A} \frac{dA}{dz}.$$

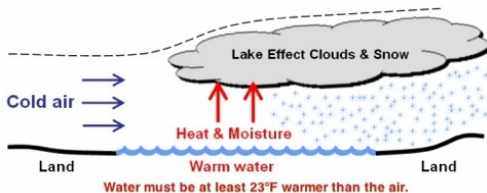


Methane ebullition from different soil columns



# Пример: снегопады над Великими Американскими озерами (lake-effect snow)

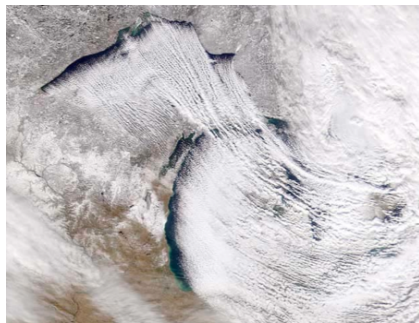
## Lake Effect Snow Conceptual Model



### "Озерные снегопады"

парализуют дорожную ситуацию, закрываются школы, отменяются полеты и т.д. В течение XX в. наблюдается тренд увеличение суммы снежных осадков в данном районе,  $+1.9 \text{ см год}^{-1}$ .

При холодных вторжениях континентального воздуха интенсивное испарение и конвекция приводят к образованию облачности и осадков.



# Example: convection over Great African Lakes

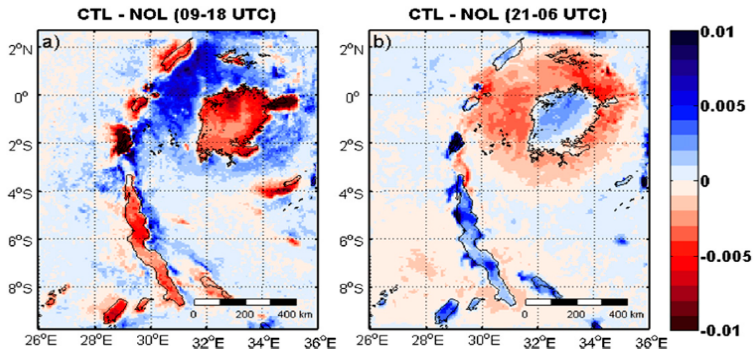
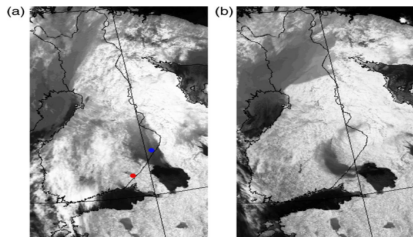


FIG. 15. The 1999–2008 mean change in convective mass flux density at cloud-base height ( $\text{kg m}^{-2} \text{s}^{-1}$ ) induced by lake presence, for (a) 0900–1800 UTC (daytime) and (b) 2100–0600 UTC (nighttime).

Nocturnal convection over Victoria accounts for annual  
fishers death toll  $\sim 5000$ .

Thiery et al. 2015, J. of Climate, DOI: 10.1175/JCLI-D-14-00565.1

## Example: cloudiness over the Ladoga Lake



*Fig. 3.* NOAA AVHRR thermal IR images over Finland and Karelia on 28 January 06 UTC (a) and on 29 January 00 UTC (b) 2012. The low-level cloud cover, shown with dark-grey shades, spreads first northward (a) and later westward (b) from Lake Ladoga. In the single-channel images, the cloud over Lake Ladoga cannot be distinguished from the dark water surfaces. The stations

Cloudiness increases the surface net radiation, and 2m-temperature rises by  $15\text{--}20^{\circ}\text{C}$

Eerola et al. Tellus A 2014, 66, 23929,  
<http://dx.doi.org/10.3402/tellusa.v66.23929>

Ice-free lake evaporates, and resulting stratiform clouds are advected to Finland.

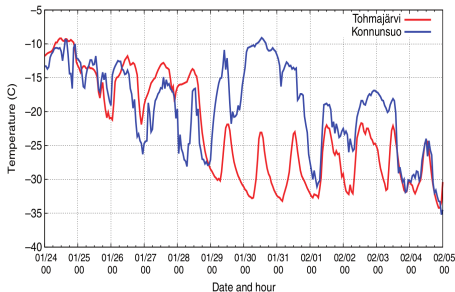
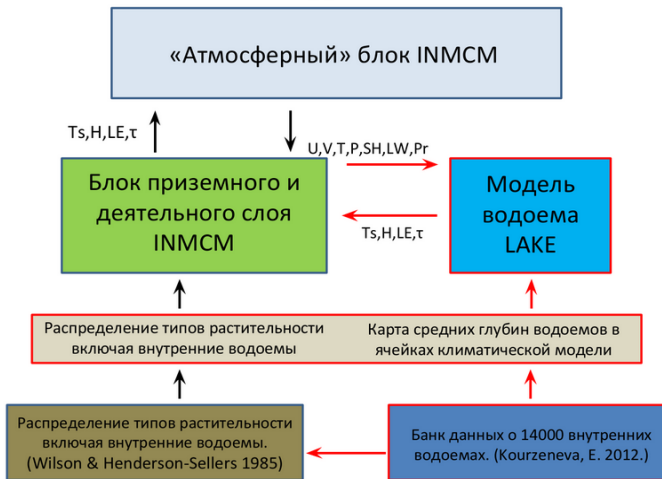
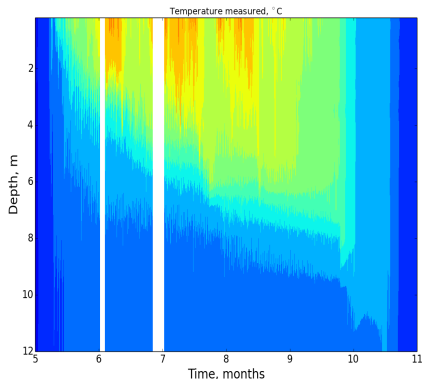


# Схема включения модели водоемов Lake в модель INMCM

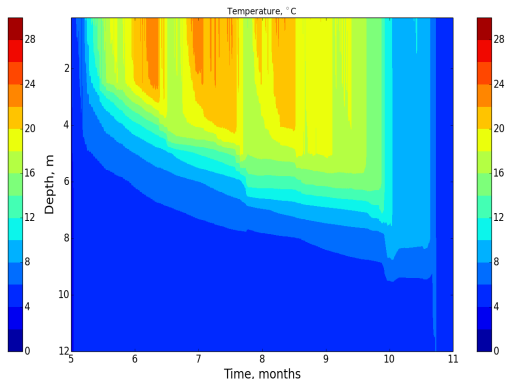


# Water temperature

Measurements



Model

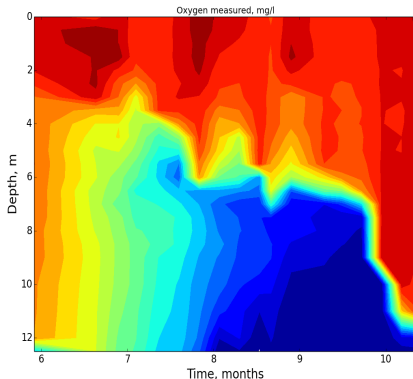


- Mixed layer depth and surface temperature (RMSE=1.54 °C) are well reproduced
- Stratification strength in the thermocline is overestimated
- Model results lack frequent temperature oscillations in the thermocline

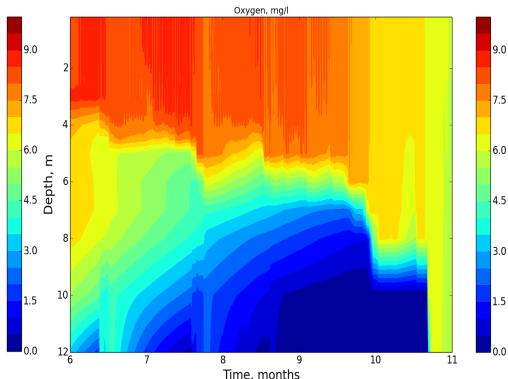
# Oxygen

Stepanenko et al., Geosci. Mod. Dev., 2016

Measurements



Model



- Seasonal pattern is well captured: oxygen is **produced** in the mixed layer and **consumed** below
- Oxygen concentration in the mixed layer is underestimated by 1-1.5 mg/l, and more significantly during autumn overturn



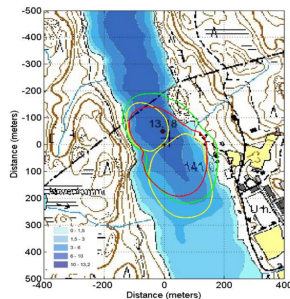
# Measurements

- Conducted since 2009 by University of Helsinki
- Ultrasonic anemometer USA-1, Metek GmbH
- Enclosed-path infrared gas analyzers, LI-7200, LI-COR Inc.
- Four-way net radiometer (CNR-1)
- relative humidity at the height of 1.5 m (MP102H-530300, Rotronic AG)
- thermistor string of 16 Pt100 resistance thermometers (depths 0.2, 0.5, 1.0, 1.5, 2.0, 2.5, 3.0, 3.5, 4.0, 4.5, 5.0, 6.0, 7.0, 8.0, 10.0 and 12.0 m)
- Turbulent fluxes were calculated from 10 Hz raw data by EddyUH software

Measurement raft

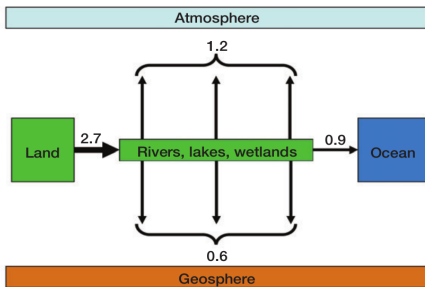


Footprint of the raft measurements



# Motivation for inclusion of rivers in ESMs

- river runoff affects thermohaline circulation
- river runoff is the most precisely measured component of the land water balance
- rivers are considered as an substantial player in land carbon cycle
- the level and ice regimes of rivers can become the one of the most in-demand output of ESMs



## H51E-1538: A global data analysis of sediment and organic carbon yield for modeling riverine biogeochemistry

Conference Paper - December 2016

Conference: AGU 2016 Fall Meeting, At San Francisco



1st Zeli Tan

at 19.17 - Pacific Northwest National Labo...



2nd L. Ruby Leung

at 45.3 - Pacific Northwest National Labor...



3rd Hongyi Li

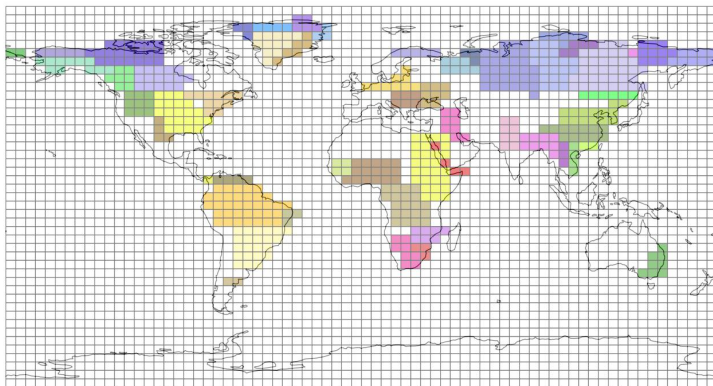
at 30.18 - Montana State University

### Abstract

Although soil erosion could have significant impacts on the global carbon cycle and the well being of aquatic and marine ecosystems, few earth system models include process-based representations of the transport of sediments and particulate organic carbon (POC) from land to rivers and streams. Two critical challenges hindering the development of such representations are scale and heterogeneity. More specifically... [\[1\]](#)

All values are in  $\text{Pg C yr}^{-1}$  (Battin et al., 2009)

# River runoff in INMCM model

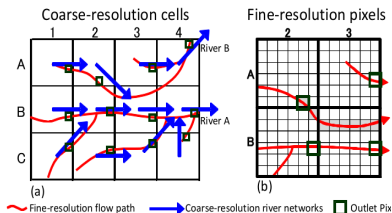


- 54 major basins
- surface and subsurface runoff are integrated over basins and instantaneously "added" to oceans in salinity equation
- no river tile in the surface energy balance calculations

# River routing for Earth System Models

Exemplified by (Yamazaki et al., 2009)

## Stream upscaling



## External parameters for river model:

- flow direction
- riverbed slope
- parameters of cross-section geometry

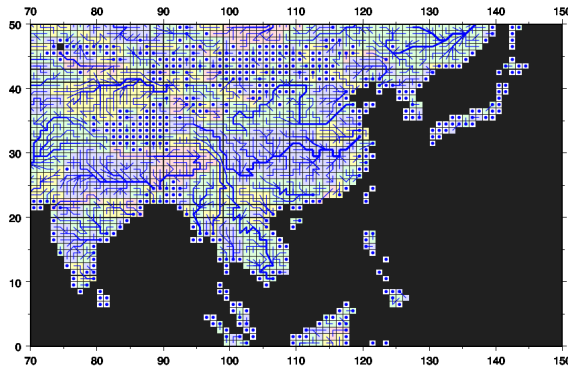


Fig. 6. Illustration of the Monsoon Asian part of an upscaled river network map at the resolution of 1 degree. Bold blue lines indicate river channels of the upscaled river network map, and circles indicate cells representing a river mouth.

# Riverflow dynamic equations

Saint-Venant system:

$$\frac{\partial S}{\partial t} + \frac{\partial SU}{\partial x} = E_r,$$

$$\frac{\partial SU}{\partial t} + \frac{\partial SU^2}{\partial x} = -g \frac{\partial(h_b + h_r)}{\partial x} - \frac{gU^2}{C^2(R)R} + \frac{\partial}{\partial x} \nu_r \frac{\partial U}{\partial x},$$

$$h_r = f(S).$$

- Highlighted are inertia terms that can be omitted if  $\text{Fr} \doteq \frac{U^2}{g(\Delta h_b + \Delta h_r)} \ll 1$
- $|\frac{\partial h_r}{\partial x}| \ll |\frac{\partial h_b}{\partial x}|$  at  $\text{Fr} < 0.1$  (Dingman, 1984)
- Longitudinal viscosity effects are also considered small

Using  $\Delta h_b = \frac{\partial h_b}{\partial x} \Delta x = s \Delta x$ , Froude number criterium becomes

$$\Delta x > \frac{10U^2}{gs} \sim 100 \text{ m for plain rivers.}$$

Under these conditions comes Manning's equation:

$$U = \frac{1}{n} R^{2/3} s^{1/2}.$$

# $k - \epsilon$ turbulence closure

$$\overline{w'\phi'} = -k_\phi \frac{\partial \bar{\phi}}{\partial z}$$

- counter-gradient effects missing

Kolmogorov formula (1942)

$$k_M = C_e \frac{E^2}{\epsilon}, \quad C_e = C_e(M, N)$$

$$k_T = k_S = C_{eT} \frac{E^2}{\epsilon}, \quad C_{eT} = C_{eT}(M, N)$$

M – friction frequency,  
N – Brunt-Vaisala frequency

stability functions

## $k-\epsilon$ parameterization

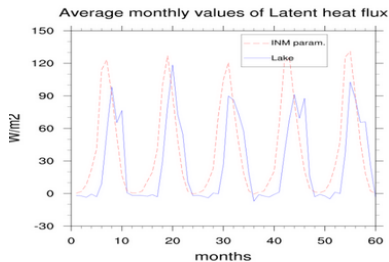
$$\frac{\partial E}{\partial t} = \frac{\partial}{\partial z} \left( v + \frac{k_M}{\sigma_E} \right) \frac{\partial E}{\partial z} + P + B - \epsilon$$

Boundary conditions

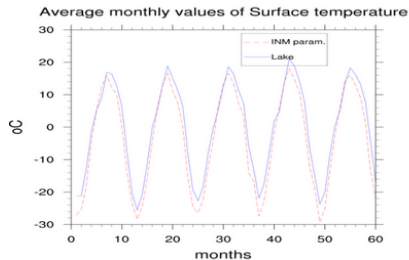
$$-\frac{k_M}{\sigma_E} \frac{\partial E}{\partial z} = c_{we} \left( \frac{\tau_s}{\rho_w} \right)^{3/2}, \quad c_{we} \approx 100$$

$$\frac{\partial \epsilon}{\partial t} = \frac{\partial}{\partial z} \left( v + \frac{k_M}{\sigma_\epsilon} \right) \frac{\partial \epsilon}{\partial z} + \frac{\epsilon}{E} (c_{1\epsilon} P + c_{3\epsilon} B - c_{2\epsilon} \epsilon)$$

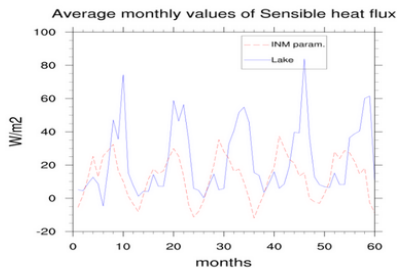
$$-\frac{k_M}{\sigma_\epsilon} \frac{\partial \epsilon}{\partial z} = (C_e^0)^{3/4} \frac{k_M}{\sigma_\epsilon} \frac{E^{3/2}}{\kappa (z' + z_0)^2}$$



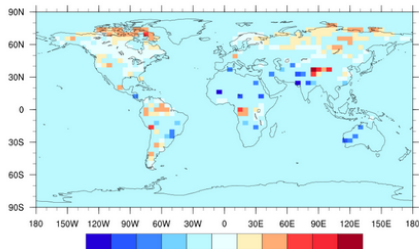
Средне месячные значения потоков скрытого тепла для озера Байкал за 5 лет



Средне месячные значения температуры поверхности для озера Байкал за 5 лет



Средне месячные значения потоков явного тепла для озера Байкал за 5 лет



Разница между среднегодовыми температурами поверхности водоемов из модели LAKE и модели INMCM